Supporting Information: Coupling Spin Defects in Hexagonal Boron Nitride to Titanium Dioxide Ring Resonators

Nonahal et. al

This supporting material includes:

1. Characterization of the deposited TiO_2 film
2. TRIM simulation of angled ion irradiation in the hBN flake
3. EDS and PL analysis of the hybrid ring resonators
4. SEM images of the fabricated hybrid ring resonators
5. Ring resonators without hBN
6. FDTD simulation
7. statistical analysis of Q-factor

SI-1: Characterization of the deposited TiO_2 film.

The Ion-assisted deposition (IAD) film morphology and optical properties were characterized by atomic force microscope and ellipsometer respectively. As shown in figure SI-1a, the derived mean surface variation, less than 4 nm and an RMS roughness of 0.9 nm, is well below the wavelength of light we invested in this work. Additionally, the TiO_2 film from IAD method was proved to exhibit a high refractive index of 2.3-2.5 in the visible to near infrared range (Figure SI-1b).

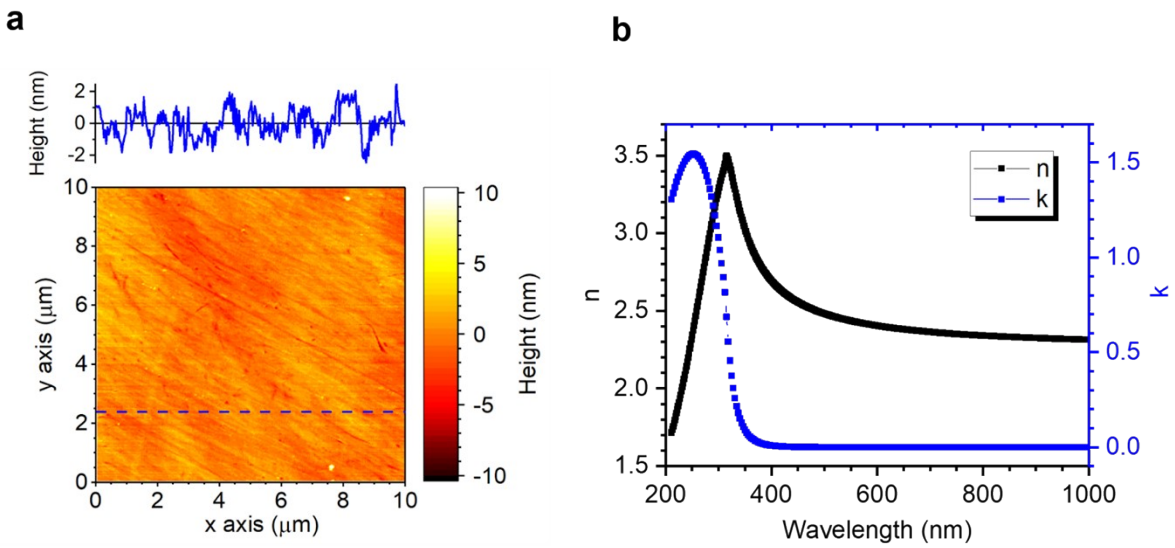

Figure SI-1. Characterization of deposited TiO_2 film. (a) AFM tomography image of the deposited TiO_2 with the mean roughness of 0.9 nm. (b) Ellipsometry analysis of the deposited TiO_2 showing refractive index of 2.3-2.5 in the visible to NIR range.

SI-2: TRIM simulation of angled ion irradiation in the hBN flake.

Monte Carlo simulation methods (TRIM) were used to determine the boron vacancy depth distribution. Here we simulated a 5 kV, N+ beam into amorphous BN (density= 2.1 g/cm3) at 60° incidence angle. Boron vacancies were almost entirely located within the 20 nm with a distribution maximum at 5 nm (figure SI-2a). To confirm thickness of prefabricated hBN flake, a AFM scanned over the patterned area as shown in figure SI-2b.

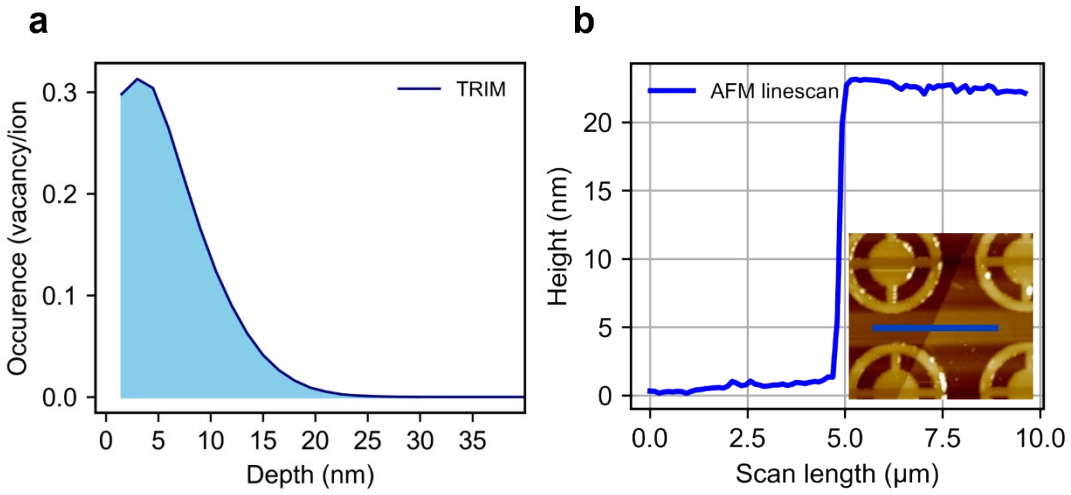

Figure SI-2. (a) TRIM simulations of boron vacancy distribution generated by 5 KeV ion energy and 60-degree angle of incident. (b) AFM profile of the prefabricated hBN flake on TiO_2 substrate. Inset shows the position of AFM linescan.

SI-3: EDS and PL analysis of the hybrid ring resonators.

The hBN/TiO_2 hybrid structure was verified by EDS and PL spectrum. Figure SI-3a to e were SEM and EDS mapping of the fabricated structure. A uniform elemental distribution of Boron, Nitrogen, Oxygen and Titanium confirm the successful fabrication of hBN/TiO_2 hybrid ring structure. Moreover, the hBN layer was confirmed by the PL measurement (figure SI-3f). The PL spectrum from the center part of the structure (red dash circle in figure SI-3a) shows two apparent peaks. In which, the 573-nm sharp peak indicates the hBN E_{2g} (1365 cm^{-1}) Raman shift under a 532-nm laser excitation along with a broad PL signal around 800 nm later confirmed by ODMR measurement. We note that the spectral range was limited by our lowest spectrometer grating to show both peaks at the same time.

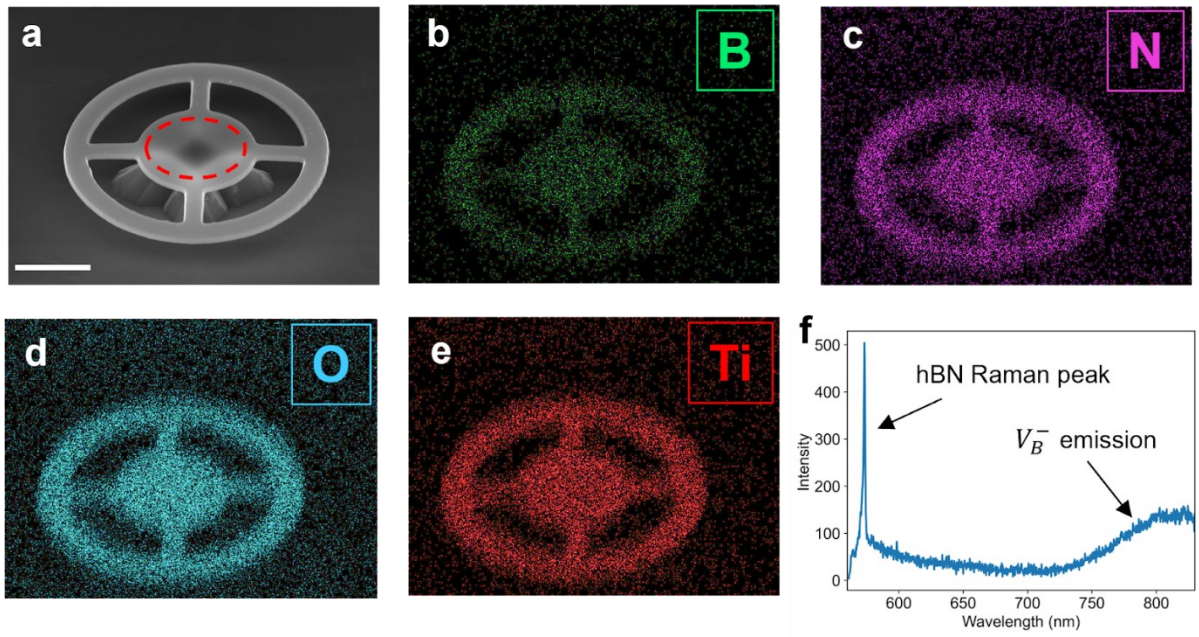

Figure SI-3. (a) Tilted SEM image of the suspended ring resonator and the corresponding EDS mapping of (b) Boron (c) Nitrogen (d) Oxygen (e) Titanium element distribution. The scale bar is 2 µm. (f) PL spectrum recorded from center of the structure as indicated by a red circle.

SI-4: SEM images of the fabricated hybrid ring resonators.

Top and side view SEM images of the fabricated sample are shown in figure SI-4. Figure SI-4a shows a tilted image of the structure after RIE and before undercut step. Vertical and smooth etching profile can be observed in the sidewall morphology of the fabricated device. To fabricate suspended structure, the underlying silicon substrate was selectively removed by KOH aqueous solution. Figure SI-4b shows an array of suspended ring resonators supported by the remaining Silicon substrate underneath the center of structure. The central disk acting as a post is directly visible from the image contrast and indicated by a yellow arrow as an aid to the eye. Magnified images of the suspended ring resonator are shown in figure SI-4c and d.

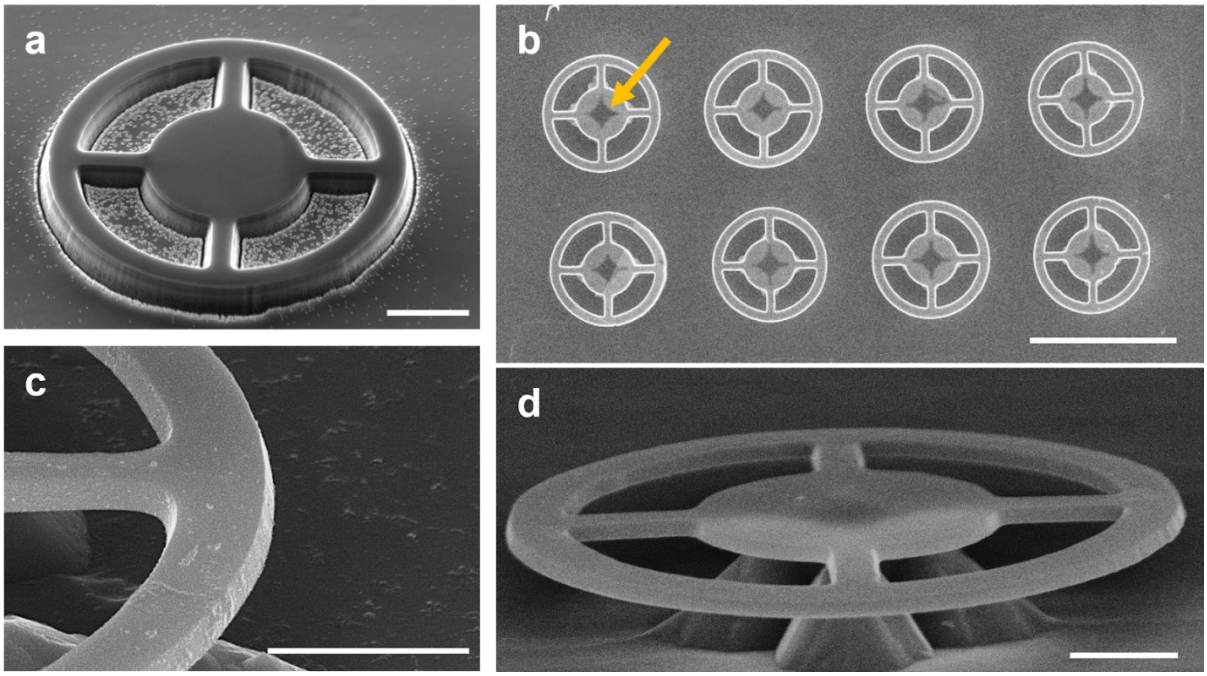

Figure SI-4. SEM images of the suspended ring resonator. (a) titled image of the RIE-etched sample prior to the undercut step. The scale bar corresponds to 2 μm. (b) Top view of an array of 8 μm ring resonators. the scale bar is 10 μm. (c) high magnification image of the sidewall of the ring resonator. The scale bar corresponds to 1 μm. (d) 70-degree tilted image of a ring resonator. The scale bar is 1 μm

SI-5: Ring resonators without hBN.

The pristine ring resonator without hBN was characterized as a reference. Background photoluminescent from polymer/contamination residuals was excited by a 6-mW green laser and signals were collected either by an APD or a spectrometer as shown in Figure SI-5a and b, respectively. A 568nm long pass filter was used to filter out the laser. The fundamental modes were observed when background photons coupled to the ring resonator and scattered out to the objective. The spectrum was recorded from the scattering point indicated by a black arrow in the PL map.

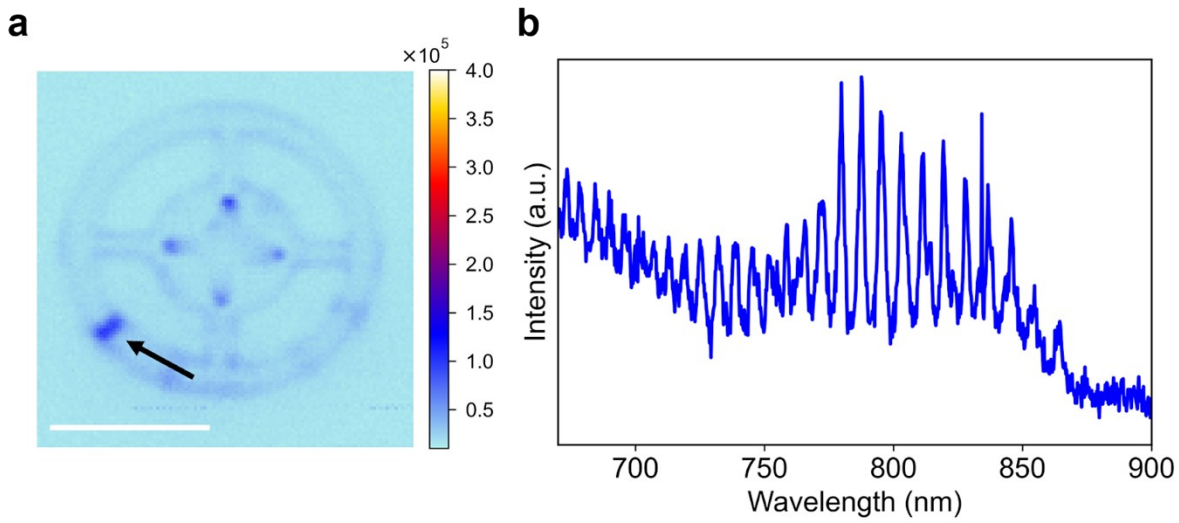

Figure SI-5. (a) PL map of the suspended ring resonator without hBN. The scale bar corresponds to 4 μm (b) PL spectrum collected from a scattering point as indicated by the arrow in the map.

SI-6: FDTD simulation.

FDTD simulation was conducted to calculate the electric field distribution of the fundamental modes of the hybrid ring resonators and the corresponding Transverse Magnetic (TM) modes and Transverse Electric (TE) modes spectra are shown in Figure SI-6.

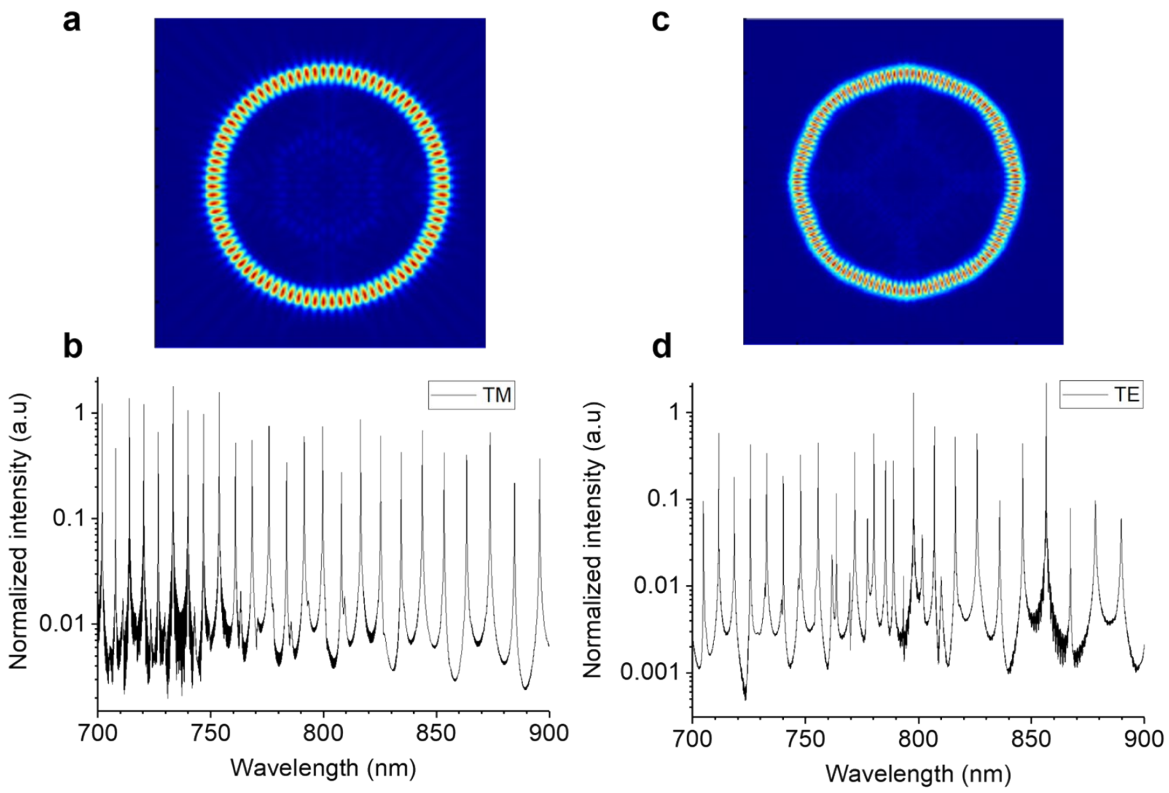

Figure SI-6. FDTD simulation of the hybrid ring resonator. TM (a) and TE (b) modes mapping and spectra (b and d).

SI-7: statistical analysis of Q-factor.

The Q-factor of an array of ring resonators was measured via a similar method as described figure 2c. Statistical analysis of the Q-factor (figure SI-7 a) shows an average of 1800 for the devices fabricated in our method. Figure SI-7 b illustrates the V_B^- enhancement for an individual coupled signal at ~790nm showing an enhancement factor of about ~14.

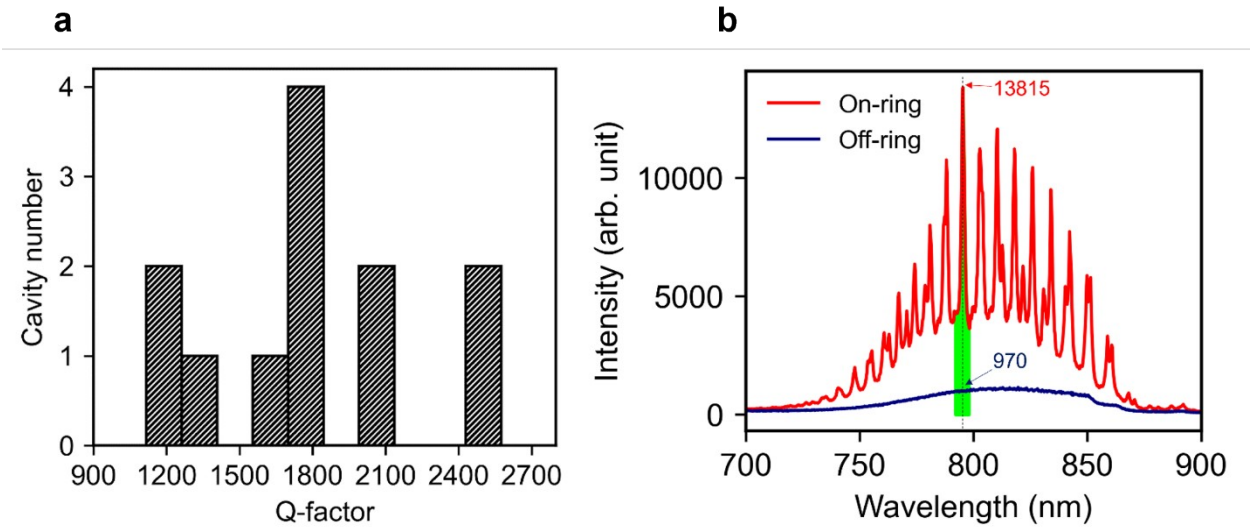

Figure SI-7. (a) statistical analysis of an array of suspended ring resonators. (b) analysis of enhancement for an individual coupled signal outlined by a green shadow. The denoted 13815 and 970 are the spectrometer counts representing the maximum intensity in coupled and uncoupled signals, respectively.